Evolutionary Ecology (2026) 40:35
https://doi.org/10.1007/s10682-026-10400-8

RESEARCH

Cyanogenesis variation in white clover is decoupled from regional climate and human footprint across a longitudinal gradient

Philips O. Akinwole[1] · Yangjie Tan[1,2] · Victor L. Alfonso[1,3]

Received: 9 February 2026 / Accepted: 11 May 2026 / Published online: 16 May 2026
© The Author(s) 2026

Abstract

Latitudinal clines in adaptive traits are well documented, yet how such patterns translate across longitudinal gradients, where climatic variation is reduced, remains poorly understood. We investigated spatial variation in hydrogen cyanide (HCN) - a well-characterized anti-herbivore defense polymorphism governed by two independently segregating loci (*Ac* and *Li*), in white clover (*Trifolium repens*) across nine Midwestern U.S. cities. A total of 269 populations (4,035 individuals) were sampled along urban-rural transects, and cyanotype (cyanogenesis phenotypes) frequencies were quantified alongside regional and site-level environmental variables, including vegetation cover (NDVI), land surface temperature (LST), snow cover, impervious surface intensity, aridity, and potential evapotranspiration. Despite substantial variation in cyanogenic frequency among cities (6.2–19.0%), minimum winter temperature varied by only 7.9 °C, markedly less than continental latitudinal gradients (21–35 °C). Accordingly, cyanogenic frequency showed no consistent relationship with environmental predictors: model selection supported a null-model, and within-city associations were heterogeneous in direction, indicating that regional effects do not scale predictably across the longitudinal gradient. In contrast, analyses of individual cyanotypes revealed locus-specific environmental associations. Site-level NDVI and LST linked to the linamarase-only cyanotype (*acLi*), suggesting increased frequency in warmer, less vegetated urban habitats. Model selection identified environmental predictors for individual cyanotypes but not for total HCN frequency. These results indicate that cyanogenesis across this regional gradient is decoupled from broad-scale climatic drivers. Instead, locus-specific responses to heterogeneous environments generate compensatory dynamics among cyanotypes, obscuring patterns at the phenotypic level. Our findings highlight the importance of genetic architecture in adaptive polymorphisms and support fine-scale selective mosaics as key drivers of evolutionary dynamics.

Keywords non-parallel adaptation · cyanogenesis · cyanotypes · minimum winter temperature · longitudinal gradient · urban evolution · white clover

Extended author information available on the last page of the article

Introduction

Urbanization is among the most pervasive and rapidly expanding drivers of global environmental change. By altering temperature, hydrology, soil chemistry, and species interactions, cities impose novel and heterogeneous selection pressures on resident organisms (Winchell et al. 2016; Rivkin et al. 2019; Alberti et al. 2020). Ecological changes driven by urbanization have the potential to significantly alter the evolutionary dynamics of populations inhabiting cities (Caizergues et al. 2022; Cosentino and Gibbs 2022; Diamond et al. 2022; Diamant et al. 2025). An expanding body of research indicates that urbanization influences both adaptive mechanisms (such as natural and sexual selection) and nonadaptive processes (including genetic drift and gene flow) across a wide diversity of organisms (Johnson and Munshi-South 2017; Santangelo et al. 2022). However, it remains unclear if evolutionary responses to urbanization are generally predictable and consistent across cities or contingent on local climatic and ecological contexts.

Recent large-scale initiatives, such as the Global Urban Evolution (GLUE) Project (*globalurbanevolution.com*), have established the value of coordinated, multi-city approaches for addressing this question (Santangelo et al. 2022; Caizergues et al. 2024; Leandro et al. 2025). The GLUE framework provides a powerful comparative foundation for detecting global patterns and local contingencies in evolutionary responses to urbanization, emphasizing the integration of ecological, genomic, and environmental data. Importantly, the GLUE project highlights that understanding adaptive evolution in urban environments directly contributes to biodiversity conservation, revealing how species persist, adapt, or decline in human-dominated ecosystems (Leandro et al. 2025).

Building on this perspective, regional-scale studies that control for key climatic variables, such as winter temperature, can clarify how non-thermal factors like hydrological stress or anthropogenic disturbance independently shape adaptive variation within cities. Longitudinal gradients, though less frequently examined than latitudinal or elevational clines, can capture meaningful environmental and historical variation that influences evolutionary dynamics independent of temperature (Conord et al. 2012; Procheş et al. 2023). Cowling et al. (2017) have drawn attention to longitudinal patterns in species diversity as ecologically relevant, reflecting variations in aridity, productivity, and disturbance rather than thermal constraints. Such studies underscore the value of longitudinal approaches for isolating non-thermal drivers of adaptation, particularly when climatic variables like minimum winter temperature (MWT) are held relatively constant.

Prior research on the perennial herb white clover (*Trifolium repens* L.*)* has demonstrated that cyanogenic polymorphism can be shaped by interacting selective pressures, including aridity, frost, and herbivory (Hughes 1991; Kooyers and Olsen 2014). However, the selective basis of this polymorphism is not universal: several studies have found limited or context-dependent evidence for selection (Wright et al. 2018, 2022; Kuo et al. 2024), suggesting that the maintenance of cyanogenic variation may reflect complex interactions among selection, genetic drift, and gene flow, the relative importance of which varies across geographic contexts. In parallel, global-scale analyses from the GLUE Project have revealed geographically widespread yet context-dependent urban-rural clines in cyanogenesis (Santangelo et al. 2022). At the global extent, Santangelo et al. (2022) tested for parallel urban-rural clines in hydrogen cyanide (HCN) frequency in white clover across 160 cities on six continents and reported widespread but context-dependent parallelism,

treating urbanization as a city-level context. Regionally, Santangelo et al. (2020) quantified urban-rural cyanogenesis clines in 15 North American cities along a latitudinal gradient (MWT range ≈ 35 °C). The present study is most comparable to that regional design, but samples nine cities along a longitudinal axis over which MWT spans only 7.9 °C and falls largely within the sub-zero thermal band where differential HCN production in *T. repens* is modest (Fadoul et al. 2023). We extend Santangelo et al. (2020) in two ways: acyanogenic individuals are resolved into *Acli*, *acLi*, and *acli* in six cities, and cyanogenesis and cyanotype frequencies are related to site-level remote-sensing predictors at 269 sites using linear mixed models with model selection. Together, these design choices allow us to ask whether non-thermal predictors can explain variation when cold-mediated selection on cyanogenesis is attenuated along the sampled corridor.

The cyanogenic polymorphism in white clover offers one of the best-characterized models for investigating adaptive evolution across environmental gradients. Cyanogenesis is a two-locus polymorphism governed by: (1) the *Ac* locus, encoding the ability to synthesize cyanogenic glucosides (stored in the vacuoles), and (2) the *Li* locus, encoding the hydrolyzing enzyme linamarase (stored in the cell wall). When both gene products are present ($Ac^{+}Li^{+}$), the plant releases hydrogen cyanide (HCN) upon tissue damage, providing chemical defense against herbivory (Hughes 1991). Other genotypes exhibit partial or complete loss of function: $Ac^{+}Li^{-}$ (*Acli*) or $Ac^{-}Li^{+}$ (*acLi*), and $Ac^{-}Li^{-}$ (*acli*) individuals are acyanogenic phenotypes (Daday 1965; Kooyers et al. 2018). Plants that produce only one component of the cyanogenic pathway may be ecologically disadvantaged, incurring the metabolic costs of cyanogenesis without gaining its defensive benefit against herbivores. However, the fitness consequences of carrying only one component are not equivalent across cyanotypes. *Acli* plants (glucosides present, enzyme absent) avoid HCN-mediated tissue damage that can occur when cellular compartmentalization is disrupted by frost or mechanical injury, while still retaining cyanogenic glucosides as nitrogen storage compounds that can be remobilized under nutrient stress (Gleadow and Møller 2014). In environments with low herbivore pressure, the absence of linamarase further eliminates expenditure on a hydrolytic system with no net defensive return. *acLi* plants (enzyme present, glucosides absent), by contrast, avoid the carbon and nitrogen costs of glucoside biosynthesis while retaining linamarase, a broad-specificity β-glucosidase with documented roles beyond HCN release, including hydrolysis of non-cyanogenic glucosides involved in cell wall metabolism and secondary compound turnover (Oxtoby et al. 1991; Barrett et al. 1995). We hypothesize that in heavily urbanized environments, where arthropod herbivore pressure is reduced (Fenoglio et al. 2020) and the defensive return on glucoside investment is therefore diminished, *acLi* plants may achieve a net fitness advantage by eliminating the biosynthetic cost of glucosides while preserving the broader metabolic utility of linamarase. The distribution of these phenotypes reflects trade-offs among defense costs, frost tolerance, and drought adaptation, producing well-documented latitudinal and altitudinal clines in cyanogenesis (Kooyers et al. 2018; Santangelo et al. 2022).

Despite this extensive foundation, the longitudinal patterns of cyanogenic variation among cities with comparable thermal climates remain poorly characterized. In this study, the longitudinal MWT gradient spanned 7.9 °C, from −15.6 °C (Sioux Falls, SD) to −7.70 °C (Indianapolis, IN), which is considerably smaller than the latitudinal gradients documented in broader geographic studies (35.36 °C in Kooyers and Olsen 2012; 35.0 °C in Santangelo et al. 2020). Importantly, experimental evidence demonstrated that the tempera-

ture dependence of HCN release in cyanogenic *T. repens* weakens at lower temperatures, approaching a plateau below approximately 15 °C (Fadoul et al. 2023), suggesting that cold-range thermal variation modulates quantitative HCN output less strongly than warmer regimes do. Our longitudinal corridor, which compresses among-city MWT variation to just 7.9 °C, therefore operates in a thermal range where temperature is expected to be a comparatively weak structuring force on cyanogenesis frequencies, motivating greater emphasis on non-thermal environmental predictors relative to continent-spanning latitudinal studies. Across most North American populations, winter cold has been identified as a key driver of HCN frequency, where northern cities with greater frost exposure harbor lower cyanogenesis frequencies than southern cities (Kooyers and Olsen 2012; Santangelo et al. 2020; Kuo et al. 2024), though it frequently covaries with other environmental factors including precipitation and aridity (Kooyers et al. 2014). The longitudinal Midwestern United States provides a unique setting to disentangle these relationships: while cities across this region share relatively similar MWT, they differ markedly in precipitation, aridity, potential evapotranspiration, and human footprint intensity. This regional environmental gradient enables testing whether urban and hydrological stressors independently shape cyanogenesis, separate from the confounding effects of continental thermal gradients.

To investigate how non-thermal environmental factors structure cyanogenesis variation independently of temperature-driven selection, we quantified cyanogenic and acyanogenic genotype frequencies across 269 populations of *T. repens* in nine Midwestern U.S. cities arranged along a longitudinal gradient where MWT variation is substantially reduced relative to continental latitudinal gradients (range = 7.90 °C, compared with ranges of 21–35 °C in broader geographic studies; Kooyers and Olsen 2012; Santangelo et al. 2020). This design allowed us to isolate the contributions of urbanization intensity, aridity, and evapotranspiration to cyanogenesis variation while holding the primary selective agent implicated in latitudinal clines (winter cold) relatively constant. We combined urban-rural transect sampling following Santangelo et al. (2020) with regional principal component analyses (PCA) of five environmental predictors: Human Footprint Index, Aridity Index, Annual Precipitation, Potential Evapotranspiration, and Minimum Winter Temperature, to contextualize broad-scale environmental variation among cities. We further extracted eight remote-sensing variables at the site level: Normalized Difference Vegetation Index in summer and winter (NDVI_summer, NDVI_winter), Land Surface Temperature in summer and winter (LST_summer, LST_winter), Normalized Difference Snow Index (NDSI), Global Man-made Impervious Surface cover (GMIS), annual Potential Evapotranspiration (PET), and Aridity Index, to address three questions: First, does HCN frequency vary predictably along urban-rural gradients independently of winter temperature variation? Second, do site-level anthropogenic and hydrological variables explain spatial variation in total cyanogenesis and individual enzyme-locus frequencies? Third, do the *Ac* and *Li* loci respond similarly to environmental gradients across cities, or do they exhibit locus-specific and context-dependent associations? We tested three sets of cyanotype-specific predictions: (i) that fully cyanogenic *AcLi* individuals would decrease with urbanization through relaxed herbivory (Johnson and Munshi-South 2017; Santangelo et al. 2022) but increase with aridity through the drought-tolerance advantage of glucoside production (Kooyers et al. 2014); (ii) that among acyanogenic cyanotypes, *Acli* individuals would increase in water-limited urban environments by retaining the glucoside-associated drought buffer without the enzymatic cost, while *acli* individuals would increase broadly with urbanization as the selective benefit

of full cyanogenesis diminishes; (iii) and that *acLi* individuals may persist in heavily urbanized environments if linamarase retains pleiotropic β-glucosidase functions independent of glucoside availability (Oxtoby et al. 1991; Barrett et al. 1995), decoupling Li-locus retention from herbivore-mediated selection. Together, these predictions reflect the expectation that urbanization restructures cyanotype frequencies differentially across the two loci rather than eroding cyanogenesis uniformly. We evaluated these predictions using a multi-step analytical framework that included null model variance partitioning, univariate and multivariate linear mixed-effects models with city as a random intercept, AICc-based model selection, random slopes heterogeneity tests, and city-level robust regressions, enabling us to distinguish globally consistent environmental effects from city-contingent ones. Together, these analyses test whether parallel urban evolution in white clover cyanogenesis reflects predictable responses to shared selective gradients or locally contingent environmental mosaics that operate independently across cities.

Materials and methods

Sampling Design

To assess whether variation in cyanogenesis in white clover is decoupled from regional climate and human footprint across a longitudinal gradient, we selected nine Midwestern cities representing a range of urban sizes, geographic locations, and climatic conditions (Fig. 1). These cities span approximately 1100 km from east (Columbus, OH) to west (Sioux Falls, SD) Midwestern USA and experience a temperature gradient from milder southeastern locations to colder northwestern cities (range = 7.9 °C; Fig. 1). The sampled cities include Columbus (OH), Indianapolis (IN), Urbana-Champaign (IL), Naperville (IL), Peoria (IL), Davenport (IA), Cedar Rapids (IA), Omaha (NE), and Sioux Falls (SD).

Sampling cities took place over two summers in three trips: trip one (May/June 2018) involved collections from Omaha and Sioux Falls; trip 2 (May 2019) from Columbus and Indianapolis; and trip three (June 2019) from Urbana-Champaign, Naperville, Peoria, Davenport, and Cedar Rapids. Our sampling protocol followed Santangelo et al. (2020) and for each city, sampling transects were established extending from urban centers through suburban zones into rural peripheries spanning a gradient of urbanization (Fig. S1a - i). In each city, we sampled fifteen *T. repens* plants from each of 26 to 31 sites (populations) (total $n = 269$ populations) spaced approximately 1 km apart, resulting in 4,035 plant samples (Table S1). Most sampling sites were in public parks, schools, athletic fields, and on lawns found along roadsides. Within each sampling site, sampled individuals were separated by at least 1.5 m to reduce the likelihood of sampling the same clonal genotype. In each site, we recorded the latitude and longitude coordinates (Table S1) and collected stolons with three to four intact leaves. Stolons were placed in plastic bags and kept in a cooler with ice until being brought back to the laboratory at DePauw University, Greencastle, IN., where they were individually placed in 2 mL microcentrifuge tubes and stored at −80 °C until HCN phenotyping.

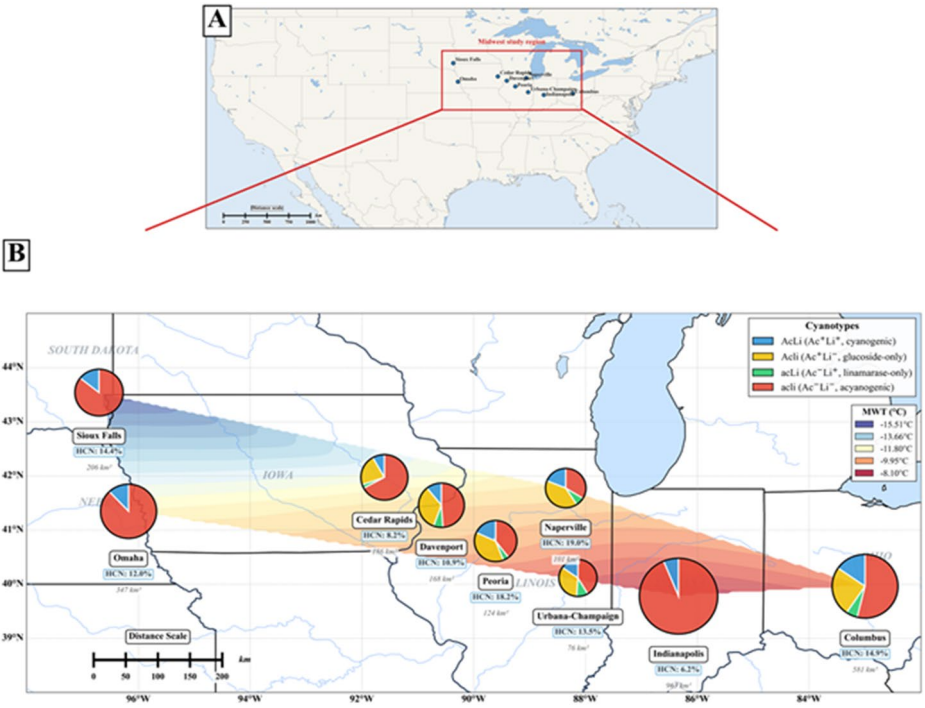


Fig. 1 Whole-USA context and Midwest study map of nine Midwestern U.S. cities showing white clover (*Trifolium repens*) populations sampled along urban-rural transects. Panel A shows the contiguous USA with the Midwest study region highlighted for geographic context. Panel B shows the nine study cities; pie charts are scaled to city land area (km²) and represent mean cyanotype frequencies averaged across all sampling populations within each city. For six cities where complementary assays were conducted (Cedar Rapids, Columbus, Davenport, Naperville, Peoria, and Urbana-Champaign), pie charts show four segments: cyanogenic *AcLi* (blue), glucoside-only *Acli* (gold), linamarase-only *acLi* (green), and fully acyanogenic *acli* (red). For three cities where only binary cyanogenesis assays were performed (Omaha, Indianapolis, and Sioux Falls), pie charts show HCN+ (cyanogenic, blue) and HCN− (acyanogenic, red) only. The map background depicts the Minimum Winter Temperature gradient (MWT, °C; WorldClim v2.1, BIO6: Minimum Temperature of Coldest Month) extracted at 30 arc-second resolution (range across 9 cities: −15.60 to −7.70 °C)

Cyanogenesis Assays

We used Feigl-Anger assays to determine whether plants were cyanogenic or acyanogenic (Feigl and Anger 1966; Gleadow et al. 2011). This assay uses a colorimetric reaction to identify plant phenotype. Briefly, microcentrifuge tubes containing leaf samples were removed from the freezer and thawed; prior freezing had lysed cells and facilitated the release of HCN. A single mature leaf from each plant was placed into a well of a 96-well plate containing 80 µL of sterile deionized water. Leaf samples were added to alternating wells, such that each plate contained 45 plant samples. Plant tissue was then macerated using pipette tips. Plates were covered with Feigl-Anger test paper and incubated at 37 °C for 3 h. We recorded a plant as cyanogenic (HCN present; i.e., $Ac^{+}Li^{+}$) if the color of the assay paper changed from white to blue, and acyanogenic (HCN absent; i.e., $Ac^{+}Li^{-}$ (*Acli*) or $Ac^{-}Li^{+}$ (*acLi)*, and $Ac^{-}Li^{-}$ (*acli*) if the color of the paper did not change. To determine the dynam-

ics of cyanogenic genotypes (individual loci underlying HCN production), all acyanogenic plants within each population of six cities (Cedar Rapids, Columbus, Peoria, Naperville, Davenport, and Urbana-Champaign) were further screened for the presence of either the *Ac* or *Li* locus using one of two complementary assays. Leaf tissue was incubated either with an exogenous cyanogenic glucoside solution to identify *acLi–* cyanotypes or with an exogenous linamarase solution to identify *Acli-* cyanotypes. Briefly, for plants that initially tested negative for HCN production, we added either (1) 40 µL of 10 mM exogenous cyanogenic glucosides (linamarin; Sigma-Aldrich 68264) plus 50 µL of deionized water, or (2) 80 µL of 0.2 EU mL^{-1} linamarase (LGC Standards CDX-00012238-100) plus 20 µL of deionized water. Samples were incubated with assay paper at 37 °C for 3 h. A positive HCN reaction in treatment (1) indicated linamarase production (*acac Li–*), whereas a positive reaction in treatment (2) indicated cyanogenic glucoside production (*Ac– lili*). Plants that showed no color change in either treatment were classified as lacking both cyanogenic glucosides and linamarase (*acac lili*). These assays have been previously validated using PCR and reliably determine cyanotypes in *T. repens* (Olsen et al. 2008; Thompson and Johnson 2016).

Regional Environmental Data and Statistical Analyses

Regional environmental data were retrieved from open databases to examine the relationship between regional abiotic factors and cyanogenesis frequencies. MWT data were extracted from WorldClim version 2.1 (BIO6: Minimum Temperature of Coldest Month) at 30 arc-second resolution from the float32 raster. Values were extracted for each GPS sampling location using bilinear interpolation. The AP values extraction procedure also utilizes high-resolution raster datasets from the WorldClim BioClim version 2.1 database (Fick and Hijmans 2017), specifically the BIO12 variable (Annual Precipitation), providing spatially explicit climate data at 30 arc-second (~1 km) resolution (https://www.worldclim.org/data/bioclim.html). We also obtained PET and AI values from global climate datasets. The extraction procedure utilizes high-resolution raster datasets from the CGIAR-Consortium for Spatial Information Global Aridity and PET Database version 3, providing spatially explicit climate data at 30 arc-second (~1 km) resolution. (Trabucco and Zomer 2019; CGIAR-CSI - https://cgiarcsi.community/data/global-aridity-and-pet-database/).

The HFI/Urban impact intensity integrates multiple anthropogenic pressures, including population density, crop and pasture lands, roads and railways, and built environments (Venter et al. 2016a). HFI was quantified with Python (Version 3.9) using the 2009 Human Footprint Index GeoTIFF dataset at 1 km^2 resolution provided by Venter et al. (2016b). HFI values were extracted using point-based nearest-neighbor sampling implemented with *rasterio.sample()* function. This method retrieves the exact pixel value at each point location without interpolation. HFI values were classified using standard categories modified from (Venter et al. 2016a) - Wilderness: $HFI < 1$ (minimal human presence); Low Impact: $1 \leq HFI < 4$ (low human modification); Moderate Impact: $4 \leq HFI < 10$ (moderate human modification); High Impact: $HFI \geq 10$ (high human modification). For city metrics, population data were obtained from 2020 U.S. Census Bureau statistics (https://www.census.gov/data.html). City land areas were compiled from official municipal records and represent incorporated city boundaries. The environmental data presented here represent city-level abiotic conditions and not the conditions extracted for each site.

To investigate whether fine-scale environmental variation contributes to city-specific cyanogenesis patterns, we extracted eight additional geospatial predictors for each of the 269 sampling sites using Google Earth Engine (GEE; Gorelick et al. 2017), calculated as the mean value within a 500 m circular buffer centered on each site's GPS coordinates. Summer and winter NDVI (NDVI_summer, NDVI_winter) were derived from the MODIS/Aqua 16-day composite (MYD13Q1, 250 m; Didan 2021) as the mean of all images acquired during June-August and December-February respectively, spanning 2018–2019. NDSI (NDSI; MOD10A2, 500 m; Hall and Riggs 2021) was averaged over December-March 2017–2019 as a proxy for frost exposure. Summer and winter Land Surface Temperature (LST_summer, LST_winter) were derived from the MODIS/Aqua 8-day product (MYD11B1, 1 km; Wan et al. 2021), averaged over June-August 2018–2019 and December-February 2017–2019 respectively. Impervious surface cover (GMIS) was obtained from the Global Human Settlement Layer built-up surface product (JRC/GHSL/P2023A/GHS_BUILT_S_10m; Pesaresi and Politis 2023), epoch 2018, and treated as an urbanization intensity index. Annual potential evapotranspiration (PET) and aridity index were additionally extracted as water-balance predictors. Prior to modelling, all eight predictors were z-score standardized globally to enable direct comparison of effect sizes across variables with different units. We fitted univariate linear mixed-effects models (LMMs) for each predictor separately (with HCN frequency as the response variable and City as a random intercept) using the model form HCN_frequency ~ Predictor_z + (1 | City). We additionally fitted a multivariate LMM including all non-collinear predictors and used AICc-based model selection (MuMIn::dredge) to identify the best-supported combination of drivers, extracting model-averaged coefficients from all models within $\Delta AICc < 2$ (full-average method). The same modelling framework was applied to acyanogenic cyanotype frequencies (*acli*, *acLi*, *Acli*) across the six cities for which complementary cyanotype assay data were available ($n = 180$ sites). Site-level models were conducted in R (vs. 4.x) using the packages lme4 (Bates et al. 2015), lmerTest (Kuznetsova et al. 2017), and MuMIn (Bartoń 2025). Marginal and conditional R^2 values were calculated using MuMIn::r.squaredGLMM following Nakagawa and Schielzeth (2013).

The map visualization was generated in Python (Version 3.9) using Matplotlib, Cartopy, and SciPy. City-level mean MWT values were interpolated across the region using cubic spline interpolation and displayed as a smooth temperature gradient with a diverging RdYlBu_r color scale. Each city is overlaid with a scaled pie chart representing the proportions of cyanogenic (HCN+, blue) and acyanogenic (HCN−, red) individuals, with pie sizes adjusted to city land area using a square-root transformation to ensure visual clarity and minimize overlap. Given that cities in this study exhibit substantial variation in transect lengths, distance was standardized between 0 and 1. The methodology employs a two-step process: (1) calculation of raw geographic distances from urban centers using the Haversine formula (Sinnott 1984), and (2) standardization of distances within each city to a 0–1 scale, where 0 represents the urban center, and 1 represents the most distant (rural) sampling point. Standardizing distance in this way allowed all transects to be on an equivalent scale, regardless of city size. To assess relationships between cyanogenesis and urban-rural distance, and between cyanogenesis and the Human Footprint Index (HFI), we fitted robust linear regressions (iteratively reweighted least squares, IRLS; Huber weights, tuning constant $k = 1.345$) for each city separately and computed Spearman rank correlations for each city and for the overall dataset. Three effects were evaluated: Distance (or HFI) Effect: whether response

variables were associated with standardized distance (or HFI) to the urban center when data were pooled across cities; City Effect: whether response variables differed among cities, regardless of distance or HFI; and Interaction: whether the relationship between distance (or HFI) and response variables differed among cities (the City × Distance or City × HFI interaction). The City × Distance interaction was formally tested via a likelihood ratio test (LRT) comparing a random-slopes linear mixed model; HCN ~ Distance + (Distance | City) - against a random-intercept model - HCN ~ Distance + (1 | City), fitted in lme4 ($\chi^2(2) = 9.53$, $p = 0.005$). Spearman rank correlations were calculated for each city and for the overall dataset to assess the strength and direction of relationships between standardized distance or HFI and the relative frequency of cyanogenesis, or cyanotypes.

To examine relationships between environmental predictors and HCN frequency across cities along longitudinal gradients, we conducted a PCA on five standardized environmental variables (HFI, MWT, AI, AP, and PET) aggregated to the city level. Environmental variables were standardized using z-score normalization to ensure equal weighting, and PCA was performed through eigenvalue decomposition of the covariance matrix. The first two PCs explained 69.5% and 23.5% of the variance in environmental predictors, respectively (cumulative: 93%), and were visualized in a biplot displaying cities as points colored by HCN frequency and environmental variables as vectors from the origin. To test for environmental effects while accounting for city-level differences, we fitted a linear mixed-effects model (LMM) with the form HCN Frequency ~ PC1 + PC2 + (1 | City), where PC1 and PC2 were included as fixed effects representing orthogonal environmental gradients, and City was included as a random intercept to account for non-independence of observations within cities. Also, for each cyanotype frequency, we fitted LMM of all environmental predictors with a random city effect of the form: Cyanotype Frequency ~ HFI + MWT + AI + AP + PET + (1 | City). Models were fitted using restricted maximum likelihood (REML), in Python using the statsmodels package, and the use of principal components as predictors avoided multicollinearity issues present among the original environmental variables.

Results

City-Specific Patterns in Hydrogen Cyanide (HCN) Frequencies along a Longitudinal Gradient

Analysis of HCN frequency across nine Midwestern U.S. cities revealed substantial spatial heterogeneity across geographic and urbanization gradients (Figs. 1 and 2). At the city scale, mean HCN frequency varied nearly threefold, from 6.2% in Indianapolis, IN, to 19.0% in Naperville, IL (Fig. 1, Table S1), with a mean HCN frequency of 12.7% (SD = 4.5%) for the nine cities, and this variation was highly significant across all models ($p < 0.001$). Importantly, HCN frequency did not follow a simple longitudinal or minimum winter temperature (MWT) gradient. Cities within similar thermal regimes exhibited contrasting frequencies [e.g., Indianapolis (6.2%) vs. Columbus (14.9%)], while colder-region cities showed moderate to high frequencies [e.g., Sioux Falls (14.4%) and Omaha (12.0%)]. Also, there was no overall relationship between HCN frequency and standardized distance from urban centers (ρ_{pool} = -0.032, $p = 0.597$; Fig. 2a). However, individual cities exhibited diverse and often strong gradient patterns, with some showing positive relationships (increasing HCN

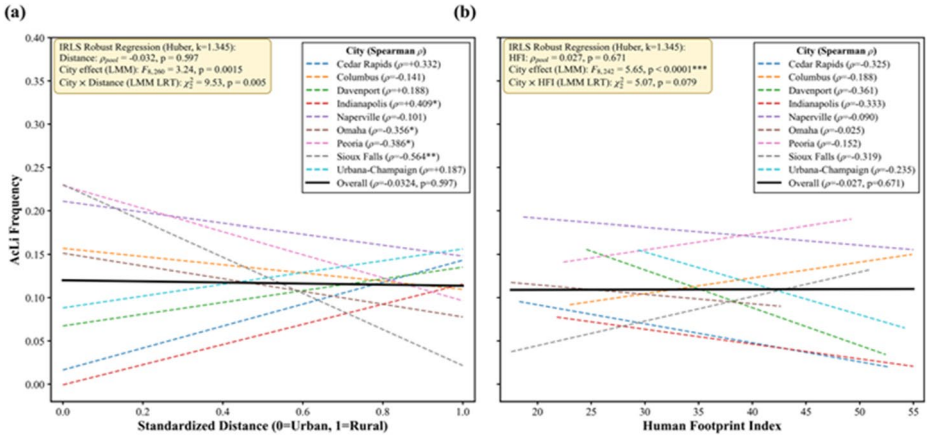


Fig. 2 Nonparallel relationships between cyanogenesis frequency and urbanization metrics across nine Midwestern U.S. cities. City-specific IRLS robust regression lines (dashed; Huber weights, k = 1.345) of *AcLi* (HCN) frequency against (a) standardized distance from the urban center (0 = urban, 1 = rural) and (b) Human Footprint Index (HFI) reveal heterogeneous and often opposing gradients among cities, with no consistent overall trend (bold solid line). Spearman ρ values per city are shown in parentheses (* $p < 0.05$, ** $p < 0.01$). Insets report pooled distance/HFI effects, city-level variance (LMM), and City × predictor interaction tests

frequency toward rural areas), e.g., Indianapolis (ρ = 0.409, $p < 0.05$), others showing negative relationships (decreasing HCN frequency toward rural areas), e.g. Omaha (ρ = -0.356, $p < 0.05$), Peoria (ρ = -0.386, $p < 0.01$) and Sioux Falls (-0.564, $p < 0.01$), and still others showing relatively flat gradients (Fig. 2a, Table S1). This heterogeneity was supported by a significant City × Distance interaction (LMM LRT: $\chi^2 = 9.53$, $p = 0.005$), implying that urban-rural gradients in cyanogenesis are highly context-dependent and shaped by local environmental or ecological factors.

Similarly, HCN frequency showed no overall relationship with the HFI ($\rho_{pool} = -0.027$, $p = 0.671$; Fig. 2b). City-specific regression lines revealed substantial heterogeneity in gradient patterns. Several cities showed negative relationships, indicating decreasing HCN frequency with increasing HFI: Cedar Rapids (ρ = -0.325), Davenport (ρ = -0.361), Indianapolis (ρ = -0.333, $p = 0.024$), Urbana-Champaign (ρ = -0.235), and Naperville (ρ = -0.090). In contrast, other cities showed positive relationships, indicating increasing HCN frequency with increasing HFI: Sioux Falls (ρ = 0.319), Columbus (ρ = 0.188), and Peoria (ρ = 0.152). Omaha exhibited a nearly flat relationship (ρ = -0.025), suggesting minimal change in HCN frequency across the HFI gradient (Fig. 2b). While individual cities differed significantly in mean HCN frequency [$F(8,242) = 5.65$, $p = 0.006$], the City × HFI interaction was not significant (LMM LRT: $\chi^2(2) = 5.07$, $p = 0.079$), indicating that city-specific HFI slopes did not vary significantly beyond what a single pooled slope would predict.

Regional Environmental Predictors of HCN Frequencies along a Longitudinal Gradient

Environmental predictors varied substantially across the nine cities (Table S2). MWT ranged from −15.60 °C (Sioux Falls, SD) to −7.70 °C (Indianapolis, OH), a range of 7.90 °C, con-

siderably smaller than the 21.36 °C and 35.0 °C MWT ranges reported in the latitudinal studies of Kooyers and Olsen (2012) and Santangelo et al. (2020), respectively. By contrast, the non-thermal predictors spanned proportionally larger gradients: Annual Precipitation (AP) ranged from 605 to 1,056 mm (range = 451 mm), the Aridity Index (AI) from 0.48 to 0.92 (range = 0.44), and Annual potential evapotranspiration (PET) from 1,146 to 1,376 mm (range = 230 mm). The HFI ranged from 15.55 in the most rural sampling sites to 55.00 in the most urbanized, a range of 39.45 units. Together, these values confirm that while temperature variation across the longitudinal gradient was reduced relative to continental latitudinal studies, substantial hydrological and anthropogenic gradients were captured, providing the environmental contrast necessary to test whether non-thermal drivers independently structure cyanogenesis variation across cities.

PCA of the five environmental variables (HFI, MWT, AI, AP, and PET) revealed that the first two PCs explained 93% of environmental variance (PC1: 69.5%, PC2: 23.5%). PC1 captured a moisture-energy balance gradient, with strong positive loadings for AI (+0.528), AP (+0.511), and moderate positive for MWT (+0.459), and a moderate negative loading for PET (-0.419) (Fig. 3, Table S3), representing a gradient from water-surplus to water-deficit environments. PC2 primarily represented variation in anthropogenic disturbance, with a strong positive loading for HFI (+0.731), capturing human impact variation independent of climate gradients. Cities were positioned in PCA space according to their environmental

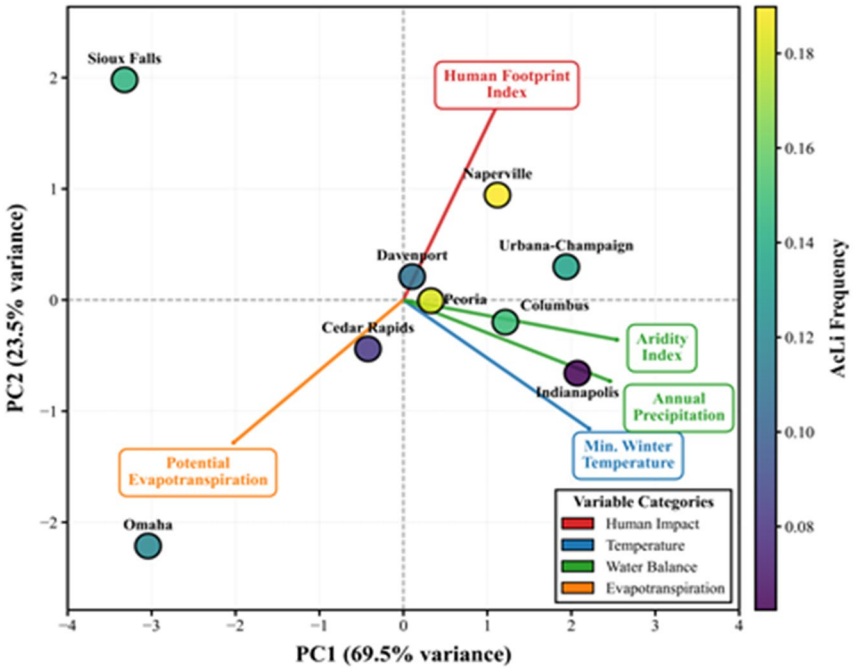


Fig. 3 Principal component analysis (PCA) summarizing environmental predictors of AcLi frequency across nine Midwestern cities. PC1 (69.5%) captures a moisture–energy balance gradient (precipitation, aridity, evapotranspiration), while PC2 (23.5%) represents human impact variation (HFI). City positions are colored by mean AcLi frequency. The lack of alignment between AcLi frequency and environmental vectors indicates that neither climate nor human footprint predicts cyanogenesis frequency, supporting city-specific, nonparallel urban evolutionary patterns

characteristics and colored by mean HCN frequency. Cities with high HCN frequencies (yellow/light green, 0.15–0.19; Naperville, Peoria, Columbus) occupied diverse positions across environmental space, spanning both high and low values of PC1 and PC2, while cities with low HCN frequencies (purple/dark blue, 0.06–0.09; Indianapolis, Cedar Rapids) also occupied varied environmental positions. For example, Naperville and Peoria, both with high HCN frequencies (~0.19 and ~0.18, respectively), occupy different positions in environmental space: Naperville is associated with high HFI and moderate climate values, while Peoria shows moderate HFI and climate values. Similarly, Indianapolis and Cedar Rapids, both with low HCN frequencies (~0.06 and ~0.08, respectively), occupy different environmental positions: Indianapolis is associated with high precipitation and temperature but moderate HFI, while Cedar Rapids shows moderate climate values and moderate HFI (Fig. 3). Furthermore, the linear mixed-effects model showed that none of the multiple environmental stressors (PC1 and PC2 as fixed effects representing environmental gradients) on longitudinal gradient was a strong predictor of mean HCN frequencies in our model (Table S4). This nonparallel pattern suggests that the same environmental conditions may lead to different HCN frequencies in different cities. Critically, analyses revealed no clear alignment between HCN frequency and environmental predictor vectors, indicating that neither the moisture-energy balance gradient (PC1) nor the human impact gradient (PC2) consistently predicted HCN frequency across cities (Fig. 3, Fig. S2).

Variation in Acyanogenic Cyanotype Frequencies along a Longitudinal Gradient

To extend our analysis beyond HCN/*AcLi* frequencies, we tested whether the relative frequencies of the three two-locus acyanogenic cyanotypes (*Acli*, *acLi*, and *acli*) varied with urbanization using the same IRLS robust regression framework applied to HCN frequency, examining within-city standardized urban-rural distance and site-level HFI as predictors. Figure S3a–f presents the corresponding scatterplots for each cyanotype-predictor combination, with city-specific data shown in color and a pooled robust fit overlaid. As with aggregate HCN frequency, these plots reveal considerable per-city scatter and locally heterogeneous trajectories rather than any uniform directional trend.

Figure 4 summarizes these patterns in tabular form, reporting for each cyanotype × predictor combination the standardized robust slope (β) on globally z-scored predictors, Wald 95% confidence intervals, two-sided Wald p-values, and a miniature forest plot on a shared β axis (dashed reference at $\beta = 0$; whiskers spanning each CI). Effect sizes were consistently small across all six tests ($|\beta| \leq \sim 0.03$). Five combinations were non-significant: pooled urban-rural distance was unrelated to *Acli*, *acLi*, or *acli* frequencies (all $p > 0.06$), and neither *Acli* nor *acli* showed meaningful associations with HFI ($p > 0.30$ and $p > 0.07$, respectively). The only significant pooled association was a modest positive relationship between *acLi* frequency and HFI ($\beta \approx +0.01$, $p \approx 0.041$), driven primarily by city-specific relationships in Columbus and Urbana-Champaign (Fig. S3e). Marginal trends ($p < 0.10$) for *acLi* versus distance and *acli* versus HFI were less precise than the aggregate HCN-urbanization signal and warrant cautious interpretation given multiple tests and dominant within-city variance. Overall, Fig. S3a–f and Fig. 4 indicate no coherent multi-city shift in acyanogenic cyanotype composition along either urbanization axis.

PCA of the environmental predictors across the six cities identified two dominant axes of environmental variation. PC1 explained 64.5% of the total variance and represented a

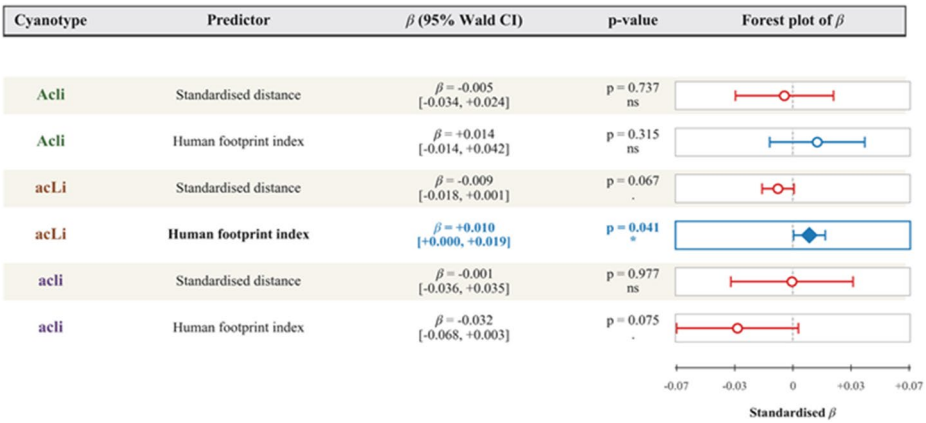


Fig. 4 Cyanotype frequencies vs. urbanization. Standardized β from IRLS robust regression (Huber weights, k = 1.345) for *Acli*, *acLi*, and *acli* on standardized distance and Human Footprint Index ($n = 181$ sites, six cities). Wald 95% CIs and p-values are tabulated; each row includes a miniature forest plot drawn on a common β axis (dashed grey line marks β = 0; whiskers span the 95% Wald CI). Only *acLi* × HFI is $p < 0.05$ (bold row). Fig. S3 lists all estimates

moisture-energy balance gradient, with strong positive loadings for AI and AP and negative loadings for PET. PC2 explained 20.9% of the variance and primarily captured variation in human impact and temperature, with positive loadings for HFI and MWT (Fig. S4). Across all three cyanotypes, cities showed no consistent alignment with either PC1 or PC2, (e.g. Naperville had the highest mean *Acli* frequency (~0.40) and Cedar Rapids the lowest (~0.22), without a consistent ordering along the moisture-energy gradient (Fig. S4), indicating that neither the moisture-energy gradient nor the combined human impact-temperature gradient strongly predicts cyanotype frequencies at the city scale. Furthermore, to test whether regional gradients explain among-city variation, we fit LMMs with city as a random intercept and all five regional predictors entered simultaneously as z-scored fixed effects (Table S5). For *Acli* and *acli* cyanotypes, none of the fixed effects was significant (all $p > 0.05$). In contrast, *acLi* exhibited significant associations with multiple climatic variables: frequency decreased with increasing AI (β = -0.674, SE = 0.275, z = -2.450, $p = 0.014$) and PET β = -0.370, SE = 0.158, z = -2.339, $p = 0.019$) and increased with higher AP (β = 0.467, SE = 0.177, z = 2.644, $p = 0.008$), whereas HFI and MWT were not significant predictors. Thus, at the city scale, multivariate moisture-energy signals are detectable for *acLi* cyanotype only, whereas *Acli* and *acli* cyanotype show no association with the same regional predictor set.

Eight geospatial predictors were extracted from Google Earth Engine and tested as site-level predictors of cyanotype frequencies using univariate LMMs. Prior to visualization, iterative VIF pruning identified aridity index (AI; VIF = 17.96) and snow cover index (NDSI; VIF = 8.63) as collinear with the retained predictor set (Fig. S5); these two variables were therefore excluded from the coefficient plot (Fig. 5). None of the six predictors was significantly associated with HCN frequency ($n = 269$ sites, nine cities; all $p > 0.19$), with the largest absolute t-statistic observed for winter NDVI (β = 0.013, SE = 0.010, t = 1.32, $p = 0.19$). For the fully acyanogenic cyanotype (*acli;* $n = 180$ sites, six cities), no predictor reached significance at α = 0.05; winter LST showed a marginal negative association (β = −0.077,

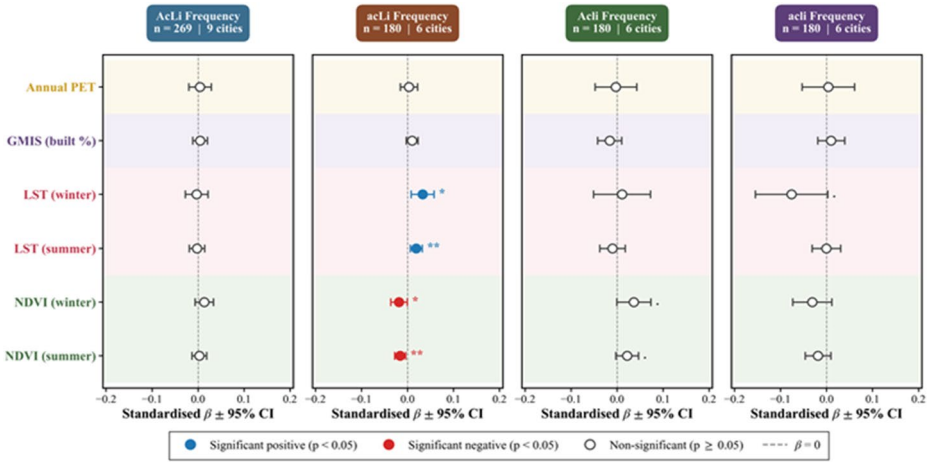


Fig. 5 Coefficient plot of standardized effect sizes of environmental predictors on AcLi/HCN frequency and acyanogenic cyanotype frequencies across Midwestern cities. Points represent standardized regression coefficients (β) with 95% confidence intervals from separate univariate linear mixed models fitted for each predictor (Model: Response ~ Predictor_z + (1 | City); REML = TRUE; Satterthwaite degrees of freedom; lme4/lmerTest). All predictors were z-score standardized using global means and standard deviations prior to model fitting ($n = 269$ sites for HCN frequency; $n = 180$ sites, 6 cities for cyanotype frequencies), enabling direct comparison of effect sizes across predictors and response variables. Only predictors retained after variance inflation factor (VIF) pruning (VIF ≤ 5) are shown; aridity index (VIF = 17.96) and snow cover index (NDSI; VIF = 8.63) were excluded due to collinearity. Filled blue circles = significant positive effect ($p < 0.05$); filled red circles = significant negative effect ($p < 0.05$); open circles = non-significant ($p \geq 0.05$). Asterisks denote significance levels (*** $p < 0.001$, ** $p < 0.01$, * $p < 0.05$). The vertical dashed line marks β = 0 (null effect). Row shading groups predictors by ecological category: green = vegetation density (NDVI), red = thermal environment (LST), purple = urbanization intensity (GMIS), amber = water balance (annual PET)

SE = 0.040, t = −1.90, $p = 0.063$), suggesting slightly higher *acli* frequencies at colder sites. For the *acLi* cyanotype (linamarase present, glucosides absent), four predictors were statistically significant: summer NDVI (β = −0.016, SE = 0.006, t = −2.69, $p = 0.0079$) and winter NDVI (β = −0.019, SE = 0.009, t = −2.08, $p = 0.039$) were both negatively associated with *acLi* frequency, whereas summer LST (β = +0.019, SE = 0.007, t = 2.84, $p = 0.0051$) and winter LST (β = +0.033, SE = 0.013, t = 2.57, $p = 0.031$) were positively associated; built-up area percentage (GMIS) and annual PET were not significant ($p = 0.131$ and 0.767, respectively). Also, a LRT favored the random-slope structure ($\chi^2 = 6.59$, df = 2, $p = 0.037$), indicating that the *acLi*–summer LST relationship varies significantly among cities. For the *Acli* cyanotype (glucosides present, enzyme absent), associations with NDVI were directionally positive but only marginally (summer NDVI: β = +0.022, SE = 0.013, $p = 0.083$; winter NDVI: β = +0.036, SE = 0.019, $p = 0.056$), with no other predictor approaching significance. The coefficient plot thus reveals a consistent pattern in which local thermal intensity and vegetation greenness (captured by LST and NDVI) align most closely with *acLi* frequency, whereas the remaining cyanotype classes and HCN frequency show limited and non-significant responses to the same site-level predictors.

Discussion

By examining cyanogenesis in white clover across a longitudinal gradient of Midwestern U.S. cities, our study tested whether urban-rural and anthropogenic gradients generate predictable adaptive patterns when winter temperature variation is minimized. Overall, we found that cyanogenic polymorphism is largely decoupled from regional climate and anthropogenic disturbance at this spatial scale. Although HCN frequency varied nearly threefold among cities (6.2–19.0%), we detected no consistent associations with standardized distance from urban centers, the HFI, or major environmental gradients summarized by PCA. These results contrast sharply with the strong and predictable latitudinal clines documented at continental scales, where temperature and aridity impose dominant selective pressures on cyanogenesis (Kooyers and Olsen 2012; Santangelo et al. 2020; Kuo et al. 2024). Rather than reflecting a weakened signal of climate-driven adaptation, our findings indicate that cyanogenic polymorphism at regional and urban scales is governed by scale-dependent, context-specific selective pressures.

Nonparallel urban-rural gradients and context dependence

A central result of this study is the strong non-parallelism in urban-rural clines of cyanogenesis across cities. While some cities exhibited positive or negative relationships between HCN frequency and distance from urban centers, others showed no detectable cline, resulting in no overall trend and a significant City × Distance interaction. Consistent with previous work, Santangelo et al. (2020) detected clines in HCN in roughly 47% of the fifteen sampled cities along a latitudinal gradient, and the GLUE project documented that the degree of parallel adaptation varied among cities (Santangelo et al. 2022). This heterogeneity demonstrates that urban-rural gradients in cyanogenesis are highly context-dependent rather than parallel across cities. Similarly, HCN frequency showed no consistent relationship with HFI, and although PCA captured substantial environmental variation related to moisture-energy balance and human impact, these gradients did not align predictably with HCN frequencies. Together, these results indicate that broad environmental metrics are poor predictors of adaptive variation at this scale.

Such nonparallel responses are increasingly recognized in urban evolutionary studies and suggest that local selective pressures, rather than shared regional gradients, dominate evolutionary outcomes in cities (Johnson and Munshi-South 2017; Rivkin et al. 2019). This pattern is further supported by our PCA results, where cities with similar HCN frequencies often occupied distinct positions in environmental space, while cities with contrasting frequencies sometimes overlapped along major environmental axes. For example, Naperville and Peoria exhibited similarly high HCN frequencies despite substantial differences in human impact and climatic characteristics, whereas Indianapolis and Cedar Rapids showed comparably low frequencies but occupied divergent environmental positions. The lack of consistent alignment between HCN frequency and either the moisture-energy gradient or the human impact gradient indicates that no single environmental axis reliably predicts cyanogenesis across cities. These findings reinforce the view that urban evolution frequently proceeds along multiple, locally contingent trajectories rather than converging on a common adaptive outcome (Liker 2020; Kemppinen et al. 2024).

Genetic architecture and local drivers of cyanogenesis

Cyanotype frequency patterns further support the dominance of local factors. For HCN frequency, this is consistent with a low null-model ICC (6.9%), indicating that most variation occurs within rather than between cities and is not structured by the measured regional or local predictors. For *Acli* and *acli*, the absence of significant site-level associations, despite directional trends in some cases, likely reflects the compressed thermal gradient of this longitudinal study (7.9 °C), which limits statistical power for detecting temperature-mediated selection, may reflect insensitivity to the environmental axes captured here, limited statistical power with six cities, or the influence of unmeasured fine-scale biotic factors.

The *acLi* cyanotype showed the most coherent environmental signal, with four predictors (NDVI_winter, NDVI_summer, LST_winter and LST_summer) reaching significance in univariate models. Critically, the opposing directionality of NDVI and LST is internally coherent: sites with higher land surface temperatures are typically more open, impervious, or thermally exposed, and are therefore associated with reduced vegetation productivity; precisely the conditions captured by lower NDVI. This convergence identifies a single ecological axis (warm, sparsely vegetated, thermally stressed microsites) as positively associated with *acLi* frequency. Two complementary mechanisms may account for this pattern. First, lower NDVI is a recognized proxy for reduced foliar biomass and associated herbivore pressure (Santangelo et al. 2022; Kooyers et al. 2014). Under the classical frequency-dependent herbivory model, fully cyanogenic plants are selectively favored where herbivore communities are more diverse and abundant (Dirzo and Harper 1982; Fadoul et al. 2023). At sparsely vegetated, low-productivity urban sites, attenuated herbivore pressure relaxes selection favoring full cyanogenesis. We hypothesize that under these conditions, *acLi* individuals, which retain linamarase, a broad-specificity β-glucosidase with documented roles beyond HCN release including hydrolysis of non-cyanogenic glucosides involved in cell wall metabolism and secondary compound turnover (Oxtoby et al. 1991; Barrett et al. 1995), may persist and increase in frequency by eliminating the biosynthetic cost of glucosides while preserving the broader metabolic utility of the enzyme, a net advantage that would be masked under high herbivore pressure where full cyanogenesis is strongly favored (Gleadow and Møller 2014). Second, higher summer and winter LST reflects thermal stress conditions under which the energetic and nitrogen investment required for cyanogenic glucoside production may be disadvantageous (Gleadow and Møller 2014). Retaining the enzyme component alone, without glucoside investment, may therefore represent an adaptive cost-saving strategy in thermally demanding, resource-limited microhabitats, consistent with the broader hypothesis that the fitness value of individual cyanogenic components is condition-dependent (Kooyers et al. 2014). The random-slopes likelihood ratio test further revealed that the positive association between *acLi* frequency and summer LST varied significantly among cities, indicating that the thermal microenvironment effect is not uniform across the urban landscape. City-specific factors, including the composition of local herbivore communities, urban heat island intensity, and the extent of impervious surface cover might modulate the strength and direction of this relationship, contributing to the among-city heterogeneity that the random-intercept model alone cannot capture.

As shown by Stuart et al. (2017), environments categorized as equivalent may differ quantitatively in selective agents; here, city-specific microclimates, frost exposure, soil moisture, and herbivore communities, among other variables (Liker 2020; Diamond et al. 2022;

Kemppinen et al. 2024) likely shift the balance of selection acting on cyanogenic versus acyanogenic genotypes. These deterministic but spatially heterogeneous selective pressures generate nonparallel genetic responses across urban landscapes rather than uniform adaptive trajectories, consistent with evidence that molecular and phenotypic responses to urban environments often lack parallelism across cities, e.g., genomic and epigenomic divergence in urban great tits, *Parus major* (Caizergues et al. 2022); nonparallel phenotypic shifts in dark-eyed juncos *Junco hyemalis* across urban sites (Diamant et al. 2025), and multi-city variation in urban-rural clines of melanism in gray squirrels (Cosentino and Gibbs 2022). Reviews of urban adaptation also emphasize that heterogeneous urban selective pressures (e.g., microclimate, pollution, biotic interactions) can produce variable evolutionary outcomes among systems (Diamond et al. 2022; Kerr et al. 2025), in line with theoretical work showing that quantitative environmental differences among replicated environments reduce the predictability of parallel evolution (Stuart et al. 2017).

Our results did not support either competing prediction for cyanotype frequency: *AcLi* plants neither declined consistently with increasing urbanization, as expected under relaxed herbivory, nor increased with aridity, as predicted from the drought-tolerance advantage of glucoside-producing genotypes. The prediction that fully acyanogenic genotypes (*acli)* would predominate in heavily urbanized, water-limited environments was similarly unsupported. Instead, the dominant signal across all analyses was city-level variance that could not be explained by the regional environmental gradients we tested, supporting the alternative hypothesis that adaptive variation in urban white clover cyanogenesis arises from locally contingent selective mosaics rather than predictable, shared responses to urbanization or aridity.

Scale dependence and the role of microclimate

The contrast between our findings and latitudinal studies highlights the importance of spatial scale in understanding adaptive evolution. Across continental gradients, cyanogenesis in white clover is strongly shaped by temperature-mediated selection, with cyanogenic plants experiencing reduced fitness in colder climates due to frost damage (Daday 1965; Hughes 1991; Kooyers and Olsen 2012). In contrast, MWT across this longitudinal gradient was restricted to a narrow inter-city band of 7.9 °C, substantially compressed relative to the 21–35 °C thermal gradients characterizing continental latitudinal studies, making temperature-mediated selection an unlikely primary driver of the HCN frequency differences observed here. In addition, unlike the wide latitudinal gradients that span ecologically distinct thermal regimes, the cities in this study share winter minima that are collectively below the temperature at which HCN production in *T. repens* responds substantially to temperature change (Fadoul et al. 2023), effectively decoupling this system from the frost-mediated selection that dominates continental-scale cyanogenesis clines. The absence of a significant MWT effect in our models is therefore consistent with the constrained thermal context of this study, and suggests that where winter temperature variation is limited, other selective agents; including urban disturbance, precipitation, and local vegetation structure may assume greater relative importance in shaping cyanotype frequencies.

Urban ecosystems generate fine-scale environmental heterogeneity through altered herbivore communities, fragmented habitats, and strong microclimatic variation driven by impervious surfaces, vegetation structure, and urban heat island effects (Liker 2020; Dia-

mond et al. 2022; Kemppinen et al. 2024). Recent work emphasizes microclimates as a critical but often underappreciated component of ecology and biogeography, capable of mediating organismal responses independently of regional climate patterns (Kemppinen et al. 2024; Kerr et al. 2025). In our system, microclimatic heterogeneity, together with variation in herbivory, soil conditions, and land-use history, likely creates locally distinct selective regimes that override regional climatic signals (Winchell et al. 2016; Diamond et al. 2022; Caizergues et al. 2024).

Implications for urban evolution and biogeography

Our findings align with and extend the GLUE framework, which predicts nonparallel evolutionary responses to urbanization driven by locally contingent selective environments (Rivkin et al. 2019; Santangelo et al. 2022). The failure of regional climate and human footprint metrics to predict adaptive variation underscores the limitations of coarse-scale environmental data for understanding fine-scale evolutionary processes in urban landscapes. From a conservation and management perspective, this suggests that adaptive variation in urban environments may be better understood and managed through city-specific approaches rather than general rules based on broad environmental gradients.

More broadly, our study contributes to a growing recognition that longitudinal sampling designs offer complementary perspectives to classical latitudinal biogeography (Procheş et al. 2023). While latitudinal gradients have been foundational for identifying broad-scale adaptive variation in cyanogenesis, including the seminal Daday effect (Daday 1965; Kooyers and Olsen 2012), they inherently conflate multiple environmental axes, including temperature, photoperiod, and precipitation (Conord et al. 2012; Procheş et al. 2023). By sampling within a comparatively narrow latitudinal band, our longitudinal design reduced thermal confounding; consistent with this, land surface temperature was not a significant predictor of HCN frequency across 269 study sites, allowing non-thermal drivers (including urban land cover and vegetation structure) to be examined more directly. We note, however, that these advantages are scale-dependent, and we make no claim that longitudinal designs are generally superior to latitudinal approaches. We encourage broader geographic replication and multi-system comparisons to assess whether longitudinal gradients consistently reveal non-thermal drivers of adaptive evolution.

By minimizing temperature variation, longitudinal gradients may function as natural experiments that help disentangle the roles of non-thermal drivers such as human disturbance, precipitation, microclimate, and local ecological interactions. While climate change is primarily driven by rising temperatures, it is also associated with shifts in precipitation regimes, increased aridity in some regions, and greater variability in hydrological extremes (AghaKouchak et al. 2020; Hansen et al. 2025). Understanding how species respond to these non-thermal dimensions of environmental change will be increasingly important for predicting evolutionary trajectories in a warming world. Furthermore, our findings provide a regional case study illustrating both the potential value and the limitations of longitudinal sampling designs in evolutionary ecology. Even when cities are well-differentiated in non-thermal environmental space (Fig. 3), cyanogenesis frequencies remain largely unpredictable from measured regional predictors, indicating that the utility of longitudinal designs for revealing adaptive patterns depends strongly on the spatial scale of the study and the resolution of environmental data available.

Limitations and conclusions

Several limitations should be considered. Although we incorporated site-level environmental surfaces from GEE in addition to regional climate and human-footprint metrics, these remain indirect proxies: they do not substitute for direct measurements of herbivory, soil moisture, frost injury, or in situ microclimate at each population, which may dominate selection on cyanogenesis at fine scales. Consequently, absence of association with a given predictor should be interpreted cautiously- it may reflect limited biological relevance of that proxy, mismatch between grain and process, or unmeasured local drivers rather than a definitive lack of environmental control. Incorporating direct measures of herbivory, microclimate, and soil properties may reveal stronger links to cyanogenesis. Additionally, our study encompassed only nine cities within a single longitudinal gradient; broader geographic sampling will be necessary to assess the generality of nonparallel urban responses. Finally, contemporary patterns may partly reflect variation in gene flow among sites, which could homogenize or differentiate cyanotype frequencies independently of local selective pressures. Importantly, we treat cyanotype-environment relationships as statistical associations, not evidence of selection, and we follow Gould and Lewontin (1979) in avoiding the assumption that every pattern reflects adaptive function. In particular, an *acLi* signal with NDVI/LST is compatible with ecological hypotheses about warm, open microsites but also with gene-flow bias, local drift in small populations, clonal structure, or indirect effects via linkage and pleiotropy. While demographic bottlenecks are unlikely given that *T. repens* shows no evidence of range-wide population contractions (Battlay et al. 2025), and past directional selection is not well-supported for cyanogenesis specifically (Wright et al. 2018, 2022; Kuo et al. 2024), spatially variable contemporary selection (for example, by frost, drought, or herbivory), remains the most parsimonious explanation for the among-city differences we observe. Disentangling these mechanisms will require direct quantification of selective agents and population connectivity, which were beyond the scope of the present study.

In conclusion, our study demonstrates that cyanogenesis variation in white clover across a longitudinal gradient of Midwestern U.S. cities is decoupled from regional climate and human footprint, with city-specific factors playing a dominant role in shaping adaptive variation. The nonparallel patterns we observed highlight the context-dependent nature of urban evolution and emphasize the importance of local ecological conditions over broad-scale environmental gradients. These findings contribute to a growing body of evidence that urban evolution is often unpredictable from regional environmental patterns alone, requiring detailed knowledge of local contexts to understand and predict adaptive responses. As urbanization continues to expand globally, understanding these local contingencies will be critical for conserving biodiversity and effectively managing urban ecosystems.

Supplementary Information The online version contains supplementary material available at https://doi.org/10.1007/s10682-026-10400-8.

Acknowledgements We appreciate the Global Urban Evolution network for providing support for the experimental design and protocols. We are indebted to DePauw alumni Seika Shiba, Anya Sanders, Spencer Golde, Kelly Garcia, and Hira Ahmad for their help with laboratory work and field collection. We thank Wendy Tomamichel, of the Chemistry Department at DePauw University, for assistance with laboratory and transportation logistics. We also thank the editor and two anonymous reviewers for their valuable comments on earlier drafts.

Author contributions POA originally formulated the idea. POA, YT and VLA conducted fieldwork and sample assays. POA analyzed the data and wrote the first draft. All authors contributed critically to several drafts through comments and revisions, and approved the final manuscript.

Funding Funding was provided by DePauw University Asher Fund in the Sciences and the Kranbuehl, Roberts, Hillger Endowed Fund for Faculty Summer Research Grant to POA.

Data availability No datasets were generated or analysed during the current study.

Declarations

Conflict of interest The authors declare no conflicts of interest.

Open Access This article is licensed under a Creative Commons Attribution 4.0 International License, which permits use, sharing, adaptation, distribution and reproduction in any medium or format, as long as you give appropriate credit to the original author(s) and the source, provide a link to the Creative Commons licence, and indicate if changes were made. The images or other third party material in this article are included in the article's Creative Commons licence, unless indicated otherwise in a credit line to the material. If material is not included in the article's Creative Commons licence and your intended use is not permitted by statutory regulation or exceeds the permitted use, you will need to obtain permission directly from the copyright holder. To view a copy of this licence, visit http://creativecommons.org/licenses/by/4.0/.

References

AghaKouchak A, Chiang F, Huning LS, Love CA et al (2020) Climate extremes and compound hazards in a warming world. Annu Rev Earth Planet Sci 48(1):519–548. https://doi.org/10.1146/annurev-earth-071719-055228

Alberti M, Correa C, Marzluff JM, Hendry AP, Palkovacs EP, Gotanda KM, Hunt VM, Apgar TM, Zhou Y (2020) Global urban signatures of phenotypic change in animal and plant populations. Proceedings of the National Academy of Sciences, 117(14), 8824–8830. https://www.pnas.org/doi/https://doi.org/10.1073/pnas.1606034114

Barrett T, Suresh CG, Tolley SP, Dodson EJ, Hughes MA (1995) The crystal structure of a cyanogenic β-glucosidase from white clover, a family 1 glycosyl hydrolase. Structure 3(9):951–960

Bartoń K (2025) MuMIn: Multi-model inference (R package version 1.48.11). CRAN. https://doi.org/10.32614/CRAN.package.MuMIn

Bates D, Mächler M, Bolker B, Walker S (2015) Fitting linear mixed-effects models using lme4. J Stat Softw 67(1):1–48. https://doi.org/10.18637/jss.v067.i01

Battlay P, Hendrickson BT, Mendez-Reneau JI, Santangelo JS, Albano LJ, Wilson J et al (2025) Haploblocks contribute to parallel climate adaptation following global invasion of a cosmopolitan plant. Nat Ecol Evol 9(8):1441–1455. https://doi.org/10.1038/s41559-025-02751-2

Caizergues AE, Luyer JL, Grégoire A, Szulkin M, Senar JC, Charmantier A, Perrier C (2022) Epigenetics and the city: Non-parallel DNA methylation modifications across pairs of urban-forest Great tit populations. Evol Appl 15(1):149–165. https://doi.org/10.1111/eva.13334

Caizergues AE, Santangelo JS, Ness RW, Angeoletto F, Anstett DN, Anstett J, Johnson MT et al (2024) Does urbanisation lead to parallel demographic shifts across the world in a cosmopolitan plant? Mol Ecol 33(7):e17311. https://doi.org/10.1111/mec.17311

Conord C, Gurevitch J, Fady B (2012) Large-scale longitudinal gradients of genetic diversity: a meta-analysis across six phyla in the Mediterranean basin. Ecol Evol 2(10):2600–2614. https://doi.org/10.1002/ece3.350

Cosentino BJ, Gibbs JP (2022) Parallel evolution of urban–rural clines in melanism in a widespread mammal. Sci Rep 12:1752. https://doi.org/10.1038/s41598-022-05746-2

Cowling RM, Bradshaw PL, Colville JF, Forest F (2017) Levyns' Law: explaining the evolution of a remarkable longitudinal gradient in Cape plant diversity. Trans Royal Soc South Afr 72(2):184–201

Daday H (1965) Gene frequencies in wild populations of Trifolium repens L. IV. Mechanism of natural selection. Heredity 20:355–365

Diamant ES, Kang M, Yeh PJ (2025) Patterns of a sexually selected trait are not predictable across urban and non-urban populations of a songbird, the dark-eyed junco. Urban Ecosyst 28:32. https://doi.org/10.1007/s11252-024-01637-8
Diamond SE, Prileson EG, Martin RA (2022) Adaptation to urban environments. Curr Opin Insect Sci 51:100893
Didan K (2021) MODIS/Aqua vegetation indices 16-Day L3 global 250m SIN grid V061. NASA EOSDIS Land Processes Distrib Act Archive Cent (DAAC) data set MYD13Q1–061. https://doi.org/10.5067/MODIS/MYD13Q1.061
Dirzo R, Harper JL (1982) Experimental studies on slug-plant interactions: III. Differences in the acceptability of individual plants of *Trifolium repens* to slugs and snails. J Ecol, 101–117
Fadoul HE, Albano LJ, Bergman ME, Phillips MA, Johnson MT (2023) Assessing the benefits and costs of the hydrogen cyanide antiherbivore defense in *Trifolium repens*. Plants 12(6):1213
Feigl F, Anger V (1966) Replacement of benzidine by copper ethylacetoacetate and tetrabase as spot-test reagent for hydrogen cyanide and cyanogen. Analyst 91:282–284
Fenoglio MS, Rossetti MR, Videla M (2020) Negative effects of urbanization on terrestrial arthropod communities: A meta-analysis. Glob Ecol Biogeogr 29(8):1412–1429. https://doi.org/10.1111/geb.13107
Fick SE, Hijmans RJ (2017) WorldClim 2: new 1-km spatial resolution climate surfaces for global land areas. Int J Climatol 37(12):4302–4315
Gleadow RM, Møller BL (2014) Cyanogenic glycosides: synthesis, physiology, and phenotypic plasticity. Annu Rev Plant Biol 65:155–185. https://doi.org/10.1146/annurev-arplant-050213-040027
Gleadow R, Bjarnholt N, Jørgensen K, Fox J, Miller R (2011) Research methods in plant science. Pp. 283–310 in S. S. Narwal, L. Szajdak, and D. A. Sampietro, eds. Soil allelochemicals. Vol. 1. Studium Press, Houston, TX
Gorelick N, Hancher M, Dixon M, Ilyushchenko S, Thau D, Moore R (2017) Google Earth Engine: Planetary-scale geospatial analysis for everyone. Remote Sens Environ 202:18–27. https://doi.org/10.1016/j.rse.2017.06.031
Gould SJ, Lewontin RC (1979) The spandrels of San Marco and the Panglossian paradigm: a critique of the adaptationist programme. Proc R Soc Lond B 205:581–598
Hall DK, Riggs GA (2021) MOD10A2 MODIS/Terra Snow Cover 8-Day L3 Global 500m SIN Grid V061. https://doi.org/10.5067/MODIS/MOD10A2.061. NASA NSIDC DAAC
Hansen JE, Kharecha P, Sato M, Tselioudis G, Kelly J, Bauer SE, Pokela A et al (2025) Global Warming Has Accelerated: Are the United Nations and the Public Well-Informed? Environment: Science and Policy for Sustainable Development, 67(1), 6–44. https://doi.org/10.1080/00139157.2025.2434494
Hughes MA (1991) The cyanogenic polymorphism in Trifolium repens L. (white clover). Heredity 66:105–115. https://doi.org/10.1038/hdy.1991.13
Johnson MT, Munshi-South J (2017) Evolution of life in urban environments. Science 358(6363):eaam8327
Kemppinen J, Lembrechts JJ, Meerbeek KV, Carnicer J, Chardon NI, Kardol P, Frenne PD et al (2024) Microclimate, an important part of ecology and biogeography. Glob Ecol Biogeogr, 33(6), e13834
Kerr JT, Gordon SC, Chen IC, Ednie G, Foden W, Newbold T, Watson MJ et al (2025) Effects of microclimate variation on insect persistence under global change. Nat Reviews Biodivers 1(8):532–542
Kooyers NJ, Olsen KM (2012) Rapid evolution of an adaptive cyanogenesis cline in introduced North American white clover (Trifolium repens L). Mol Ecol 21:2455–2468
Kooyers NJ, Gage LR, Al-Lozi A, Olsen KM (2014) Aridity shapes cyanogenesis cline evolution in white clover (T rifolium repens L). Mol Ecol 23(5):1053–1070
Kooyers NJ, Hartman Bakken B, Ungerer MC, Olsen KM (2018) Freeze-induced cyanide toxicity does not maintain the cyanogenesis polymorphism in white clover (Trifolium repens). Am J Bot 105(7):1224–1231. https://doi.org/10.1002/ajb2.1134
Kuo WH, Zhong L, Wright SJ, Goad DM, Olsen KM (2024) Beyond cyanogenesis: Temperature gradients drive environmental adaptation in North American white clover (Trifolium repens L). Mol Ecol 33(17):e17484. https://doi.org/10.1111/mec.17484
Kuznetsova A, Brockhoff PB, Christensen RHB (2017) lmerTest package: Tests in linear mixed effects models. J Stat Softw 82(13):1–26. https://doi.org/10.18637/jss.v082.i13
Leandro D, Johnson MT, Schneider AC, Lázaro-Lobo A, Caizergues AE, Lara C, Akinwole PO, Angeoletto F et al (2025) GLUEing the world: The GLobal urban evolution project and its importance to urban biodiversity conservation. Ecology of Tropical Cities, Volume I: Natural and Social Sciences Applied to the Conservation of Urban Biodiversity. Springer, Cham, pp 217–230. https://doi.org/10.1007/978-3-031-48012-6_12Nature Switzerland
Liker A (2020) Adaptive changes in urban populations. Biol Futura 71:1–8. https://doi.org/10.1007/s42977-020-00005-9

Nakagawa S, Schielzeth H (2013) A general and simple method for obtaining R^2 from generalized linear mixed-effects models. Methods Ecol Evol 4(2):133–142. https://doi.org/10.1111/j.2041-210x.2012.00261.x

Olsen KM, Hsu SC, Small LL (2008) Evidence on the molecular basis of the Ac/ac adaptive cyanogenesis polymorphism in white clover (Trifolium repens L). Genetics 179:517–526. https://doi.org/10.1534/genetics.107.080366

Oxtoby E, Dunn MA, Pancoro A et al (1991) Nucleotide and derived amino acid sequence of the cyanogenic β-glucosidase (linamarase) from white clover (Trifolium repens L). Plant Mol Biol 17:209–219. https://doi.org/10.1007/BF00039495

Pesaresi M, Politis P (2023) GHS-BUILT- S R2023A — GHS built-up surface grid, derived from Sentinel2 composite and Landsat, multitemporal (1975–2030). Eur Comm Joint Res Centre (JRC). https://doi.org/10.2905/9F06F36F-4B11-47EC-ABB0-4F8B7B1D72EA

Procheş Ş, Watkeys MK, Ramsay LF, Cowling RM (2023) Why we should be looking for longitudinal patterns in biodiversity. Front Ecol Evol 11:1032827. https://doi.org/10.3389/fevo.2023.1032827

Rivkin LR, Santangelo JS, Alberti M, Aronson MFJ, Keyzer CD, Diamond SE, Fortin MJ, Frazee LJ, Gorton AJ, Hendry AP, Liu Y, Losos JB, MacIvor JS, Martin RA, Munshi-South J, Ness RW, Newman AEM, Stothard P, Thompson KA, Johnson MTJ et al (2019) A roadmap for urban evolutionary ecology. Evol Appl 12(3):384–398. https://doi.org/10.1111/eva.12734

Santangelo JS, Thompson KA, Cohan B, Syed J, Ness RW, Johnson MT (2020) Predicting the strength of urban-rural clines in a Mendelian polymorphism along a latitudinal gradient. Evol Lett 4(3):212–225. https://doi.org/10.1002/evl3.163

Santangelo JS, Ness RW, Cohan B, Fitzpatrick CR, Innes SG, Koch S, Lampei C et al (2022) Global urban environmental change drives adaptation in white clover. Science 375(6586):1275–1281

Sinnott RW (1984) Virtues of the Haversine. Sky Telescope 68(2):159

Stuart YE, Veen T, Weber JN, Hanson D, Ravinet M, Lohman BK et al (2017) Contrasting effects of environment and genetics generate a continuum of parallel evolution. Nat Ecol Evol 1:1–7. https://doi.org/10.1038/s41559-017-0158

Thompson KA, Johnson MTJ (2016) Antiherbivore defenses alter natural selection on plant reproductive traits. Evolution 70:796–810. https://doi.org/10.1111/evo.12900

Trabucco A, Zomer R, CGIAR-CSI (Consultative Group on International Agricultural Research - (2019) Global aridity index and potential evapotranspiration (ET0). Climate Database v22019, 10. Consortium for Spatial Information). https://cgiarcsi.community/data/global-aridity-and-pet-database/

Venter O, Sanderson EW, Magrach A, Allan JR, Beher J, Jones KR et al (2016a) Sixteen years of change in the global terrestrial human footprint and implications for biodiversity conservation. Nat Commun 7:12558. https://doi.org/10.1038/ncomms12558

Venter O, Sanderson EW, Magrach A, Allan JR, Beher J, Jones KR, Watson JE et al (2016b) Global terrestrial Human Footprint maps for 1993 and 2009. Sci data 3(1):1–10. https://doi.org/10.1038/sdata.2016.67

Wan Z, Hook S, Hulley G (2021) MODIS/Aqua Land Surface Temperature/Emissivity Daily L3 Global 6km SIN Grid V061. NASA EOSDIS Land Processes Distrib Act Archive Cent (DAAC) data set MYD11B1–061. https://doi.org/10.5067/MODIS/MYD11B1.061

Winchell KM, Reynolds RG, Prado-Irwin SR, Puente-Rolón AR, Revell LJ (2016) Phenotypic shifts in urban areas in the tropical lizard Anolis cristatellus. Evolution 70(5):1009–1022. https://doi.org/10.1111/evo.12925

Wright SJ, Cui Zhou D, Kuhle A, Olsen KM (2018) Continent-wide climatic variation drives local adaptation in North American white clover. J Hered 109(1):78–89. https://doi.org/10.1093/jhered/esx060

Wright SJ, Goad DM, Gross BL, Muñoz PR, Olsen KM (2022) Genetic trade-offs underlie divergent life history strategies for local adaptation in white clover. Mol Ecol 31(14):3742–3760. https://doi.org/10.1111/mec.16180

Publisher's note Springer Nature remains neutral with regard to jurisdictional claims in published maps and institutional affiliations.

Authors and Affiliations

Philips O. Akinwole[1] · Yangjie Tan[1,2] · Victor L. Alfonso[1,3]

✉ Philips O. Akinwole
philipsakinwole@depauw.edu

[1] Biology Department, DePauw University, Greencastle, IN 46135, USA

[2] Biomedical Engineering Department, Washington University in Saint Louis, Saint Louis, MO 63105, USA

[3] Aytu Biopharma Inc, Columbus, OH, USA